

**Figure 5** Shows a schematic diagram of magnetic field (current), where the Au is the coated material. [Color figure can be viewed in the online issue, which is available at [wileyonlinelibrary.com](http://wileyonlinelibrary.com)]

in which the tunneling photons can be generated and confined within a center ring by the WGMs. In application, the coupling effects between the WGMs and physical environments can be detected by the device drop port output, which can be related to the required measurements, therefore, the changes in wavelength(s) (or phases) of the WGMs (center signals) obtained by the sensing unit can be retrieved and interpreted. In this article, three forms of sensing configurations are proposed by using the WGMs within the PANDA ring circuits, where the sensing configurations such as microflow rate sensors, thin film and distributed sensors and wrist band for medical sensors are proposed. Furthermore, the use of a coated PANDA ring can also give more widely applications, which can be used for magnetic and current sensing forms as shown in Figure 5, which is shown that the trapping and moving electron along the center of ring, which is coated with Au and produce the propagation of magnetic field around the ring as shown in Figures 5(a.1) and 5(a.2), so-called nanosolenoid, which is formed by the surface plasmon concept. For sensing applications, magnetic fields (B) or currents (I) can be changed relatively to the environmental environments and configured to be the required sensors.

### 3. CONCLUSION

We have proposed the very interesting sensing configurations using the concept of nonlinear coupling effects within a PANDA ring circuit and WGMs of light. The coupling effects between the WGMs and external environments can be detected and measured related to the shift in phase, that is, WGMs phase (position in the time or wavelength domains). The large area sensing application is also available when the distributed sensing configuration is used. Moreover, in some cases light can penetrate into human tissue using the WGMs switching control, which can be useful for medical sensing applications.

### ACKNOWLEDGMENT

The authors would like to give the acknowledgement to King Mongkut's Institute of Technology Ladkrabang (KMUTL), Bangkok 10520, Thailand for the laboratory facilities.

### REFERENCES

1. D.J. Wineland, J.J. Bollinger, W.M. Itano, and J.D. Prestage, Angular momentum of trapped atomic particles, *J Opt Soc Am B* 2 (1985), 1721–1730.
2. J.C. Knight, N. Dubreuil, V. Sandoghdar, J. Hare, V. Lefevre-Seguin, J.M. Raimond, and S. Haroche, Characterizing whispering-gallery modes in microspheres by direct observation of the optical standing-wave pattern in the near field, *Opt Lett* 21 (1996), 698–670.
3. N. Sarapat, W. Khunnam, S. Chiangga, N. Thammawongsa, M.A. Jalil, J. Ali and P.P. Yupapin, Fast, slow, stopping and storing light

simultaneously using a PANDA ring on-chip, *Asia Pac Phys News* 2 (2013), 37–39.

4. V.M.N. Passaro and F. De Leonardis, Modeling and design of a novel high-sensitivity electric field silicon-on-insulator sensor based on a whispering-gallery-mode resonator, *IEEE J Sel Top Quantum Electron* 12 (2006), 124–133.
5. T. Iopolo, N. Das, and M.V. Otugen, Whispering gallery modes of microspheres in the presence of a changing surrounding medium: A new ray-tracing analysis and sensor experiment, *J Appl Phys* 107 (2010), 103105–103108.
6. I. Teraoka and S. Arnold, Dielectric property of particles at interface in random sequential adsorption and its application to whispering gallery mode resonance-shift sensors, *J Appl Phys* 101 (2007), 023505–023509.
7. P. Zijlstra, K.L. van der Molen, and A.P. Mosk, Spatial refractive index sensor using whispering gallery modes in an optically trapped microsphere, *Appl Phys Lett* 90 (2007), 161101–161103.
8. J.M. Gamba and R.C. Flagan, Flow-enhanced transient response in whispering gallery mode biosensors, *Appl Phys Lett* 99 (2011), 253705–253708.
9. P.P. Yupapin, Nonlinear coupling effects of waves in a PANDA ring, *Sci Discov* 1 (2013), 1–5.
10. P.P. Yupapin and S. Nimcome, Conjugate mirror by a PANDA ring circuit, *Sci Innov* 1 (2013), 1–4.
11. N. Tmammawongsa, S. Tunsiri, M.A. Jalil, J. Ali, and P.P. Yupapin, Storing and harvesting atoms/molecules on-chip: challenges and applications, *Biosens Bioelectron* 3 (2012), e114–e115.
12. J.C. Knight, N. Dubreuil, V. Sandoghdar, J. Hare, and V. Lefevre-Seguin, Characterizing whispering-gallery modes in microspheres by direct observation of the optical standing-wave pattern in the near field, *Opt Lett* 21 (1996), 698–670.
13. K. Uomwech, K. Sarapat, and P. P. Yupapin, Dynamic modulated Gaussian pulse propagation within the double PANDA ring resonator system, *Microwave Opt Technol Lett* 52 (2010), 1818–1821.
14. OptiFDTD by Opti-wave Corporation Company, Version 8.0, single license, 2006.

© 2014 Wiley Periodicals, Inc.

## FOUR-PORT BALANCED ANTENNA FEEDING NETWORK FOR SWITCHABLE POLARIZATIONS AND STABLE TX/RX ISOLATION CHARACTERISTICS

Han-Lim Lee,<sup>1</sup> Dong-Hoon Park,<sup>2</sup> Hyun-Sung Tae,<sup>1</sup> Moon-Que Lee,<sup>2</sup> and Jong-Won Yu<sup>1</sup>

<sup>1</sup>School of Electrical Engineering and Computer Science, Korea Advanced Institute of Science and Technology, 373-1 Guseong-Dong, Yuseong-Gu, Daejeon, South Korea

<sup>2</sup>School of Electrical Engineering and Computer Science, University of Seoul, 90 Jeonnong-Dong, Dongdaemun-Gu, Seoul, South Korea; Corresponding author: [mqllee@uos.ac.kr](mailto:mqllee@uos.ac.kr)

Received 28 April 2013

**ABSTRACT:** A new four-port balanced antenna feeding network for switchable polarizations and high transmit/receive (Tx/Rx) isolation characteristics is presented. The proposed structure is configured by two switching mode hybrid matrices which consist of two 3-dB couplers and two SP4T switches, two directional couplers, and Wilkinson dividers. By controlling impedances of the switching mode hybrid matrices, different types of polarizations such as right-handed circular polarization, left-handed circular polarization, vertical polarization, and horizontal polarization can be generated with stable Tx/Rx isolation characteristics regardless of antenna impedance variations. © 2014 Wiley Periodicals, Inc. *Microwave Opt Technol Lett* 56:17–23, 2014; View this article online at [wileyonlinelibrary.com](http://wileyonlinelibrary.com). DOI 10.1002/mop.27991

**Key words:** antenna feeding network; reconfigurable feeding network; Tx/Rx isolation; reconfigurable antenna

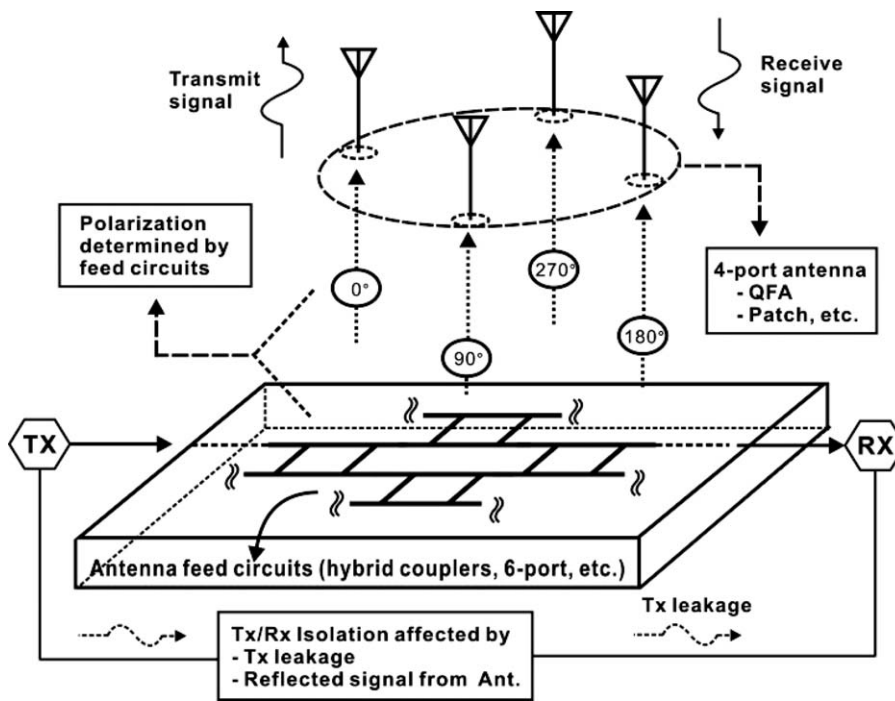


Figure 1 Antenna front-end structure for polarization and Tx/Rx isolation

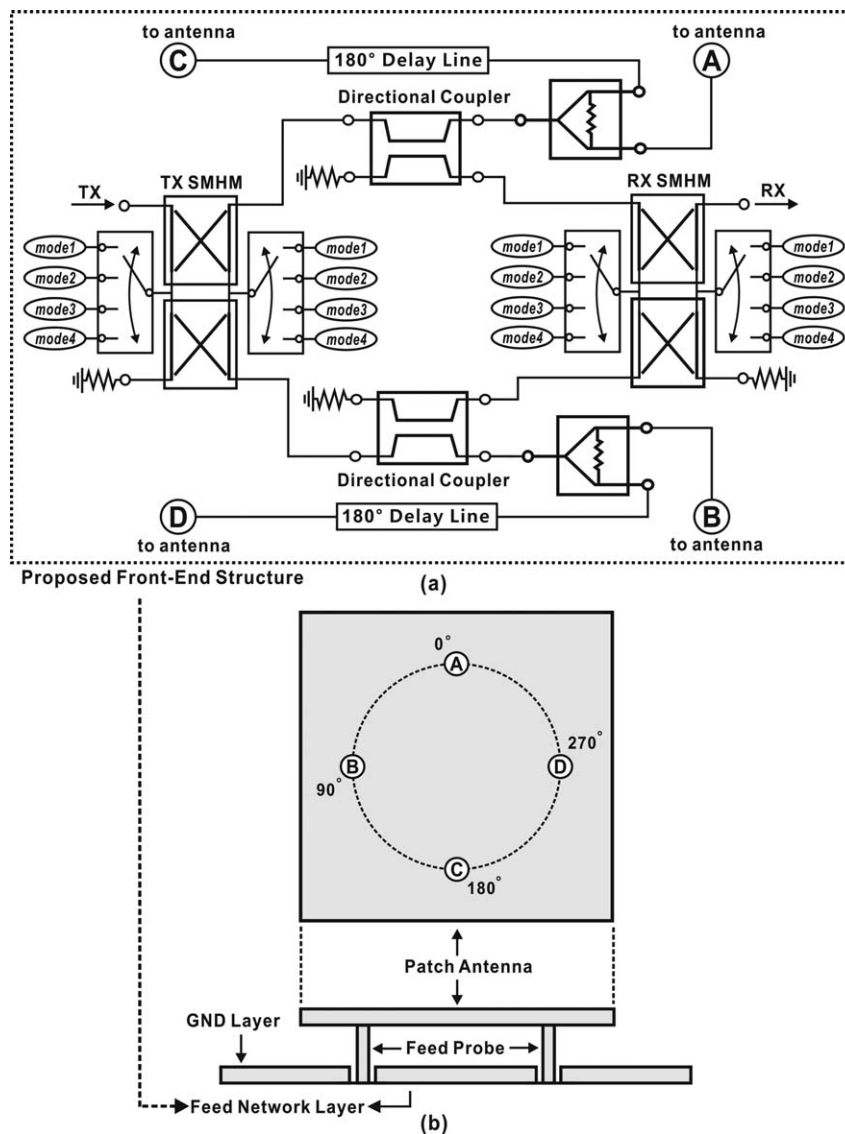
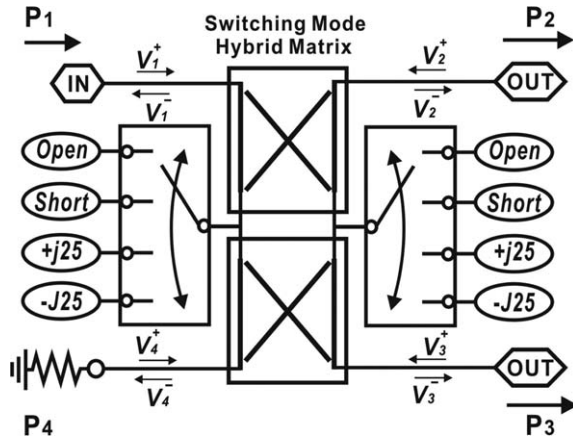


Figure 2 Block Diagram for: (a) the proposed balanced antenna feeding network and (b) its application to a patch antenna



**Figure 3** Switching mode hybrid matrix for feed path control

**1. INTRODUCTION**

Antenna feeding network takes a very important role in multiport antenna front-end structures as transmit/receive (Tx/Rx) antenna polarizations and isolation characteristics are determined by the feeding networks as illustrated in Figure 1. The feeding network makes different signal magnitudes and phases at each antenna feeding point and corresponding polarizations are generated for Tx and Rx. For a single antenna system, as Tx and Rx share the same antenna and feeding networks are usually separated by passive circuits, the isolation characteristic between Tx and Rx is very crucial regarding receiver performances. Thus, the unwanted signals such as Tx leakage and antenna reflection

should also be taken into account as well as antenna polarizations when feeding network is designed.

In order to cancel Tx leakages, there have been researches such as Doppler radar applications using quadrature hybrids and Lange couplers [1–3], but these structures are valid only in a well-matched conditions and polarizations are fixed and not switchable. To remove the Tx leakage and antenna reflection regardless of the antenna impedance variations, balanced antenna front-end structures [4, 5] have also been proposed, but polarizations are fixed and cannot be controlled. Thus, in this article, we propose a new antenna feeding network that can provide controllable polarizations (right-handed circular polarization (RHCP), left-handed circular polarization (LHCP), vertical polarization (VP), and LP) and maintain high isolation characteristics for Tx and Rx independent of polarizations and antenna impedance variations. The Tx and Rx polarizations can be controlled separately by switching mode hybrid matrices and high Tx/Rx isolation can be retained when Tx/Rx circular polarizations are set equally or Tx/Rx linear polarizations are set differently. For instance, high and stable Tx/Rx isolation characteristics can be achieved by RHCP (LHCP) for both Tx and Rx as well as LP (VP) for Tx and VP (LP) for Rx.

**2. FOUR-PORT BALANCED ANTENNA FEEDING NETWORK**

*2.1. Analysis for Switching Mode Hybrid Matrix*

Figure 2 shows the proposed four-port balanced antenna feeding network and its application to a generally used four-port patch antenna. The proposed structure is configured by two switching mode hybrid matrices which consist of two 3-dB couplers and two SP4T switches, two directional couplers, and Wilkinson dividers (combiners). Each switching mode hybrid matrix sets

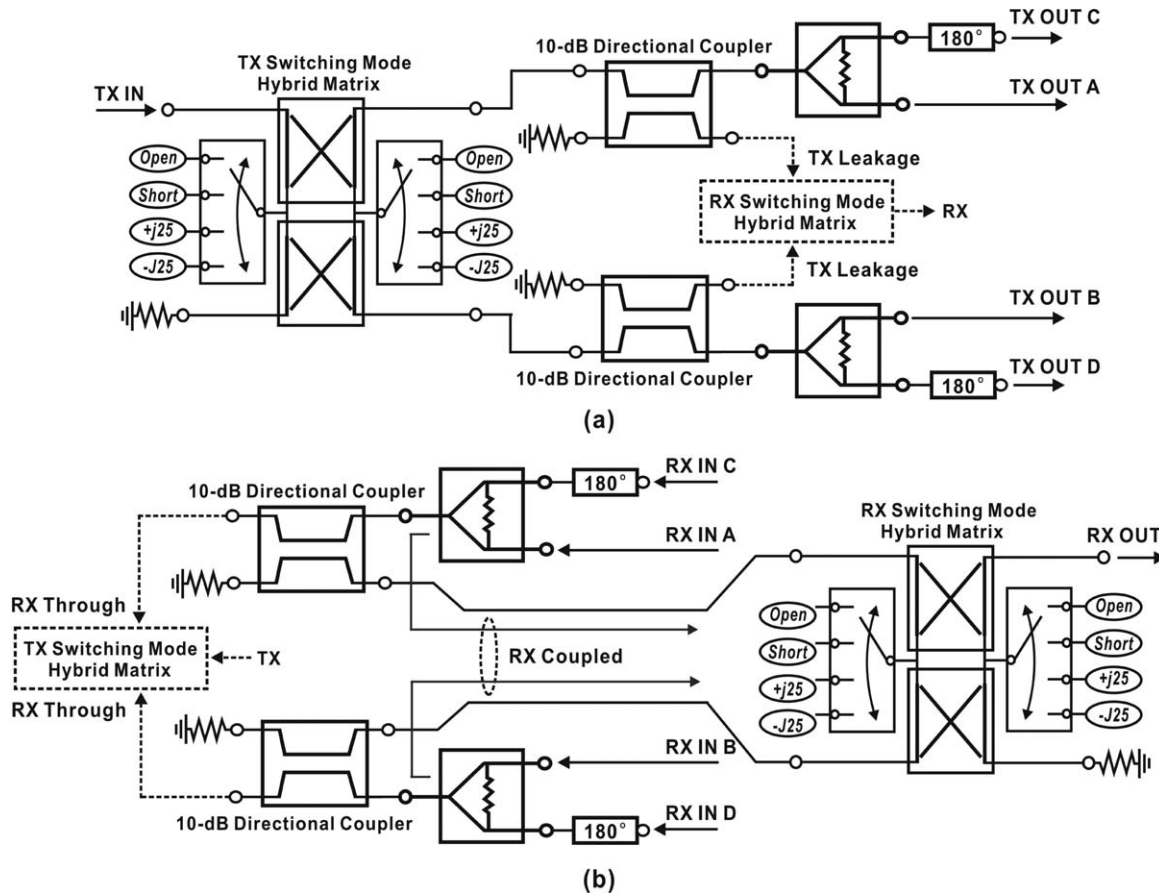


**Figure 4** Operation of the proposed antenna feeding network for: (a) Tx and (b) Rx

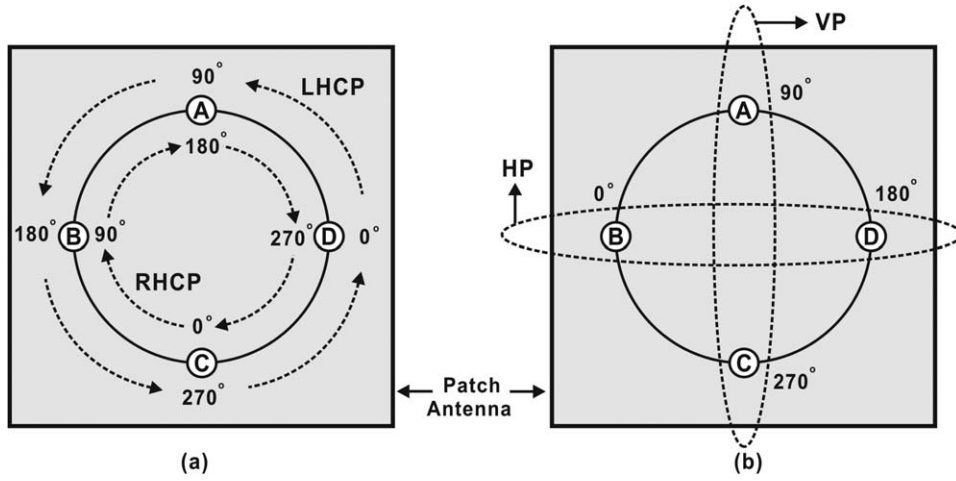


**Figure 5** Polarization of a patch antenna generated by the proposed antenna feeding network: (a) CP and (b) LP

**TABLE 1** Summary of the Tx Polarizations According to Switch Modes

Switch Mode	Open	Short	+j25 Ω	-j25 Ω
Tx out A	0	$\frac{1}{2} e^{-j\theta+\pi/2}(90^\circ)$	$\frac{1}{2} e^{-j\theta+\pi}(180^\circ)$	$\frac{1}{2} e^{-j\theta+\pi/2}(90^\circ)$
Tx out B	$\frac{1}{2} e^{-j\theta+\pi}(180^\circ)$	0	$\frac{1}{2} e^{-j\theta+\pi/2}(90^\circ)$	$\frac{1}{2} e^{-j\theta+\pi}(180^\circ)$
Tx out C	0	$\frac{1}{2} e^{-j\theta+3\pi/2}(270^\circ)$	$\frac{1}{2} e^{-j\theta+2\pi}(0^\circ)$	$\frac{1}{2} e^{-j\theta+3\pi/2}(270^\circ)$
Tx out D	$\frac{1}{2} e^{-j\theta+2\pi}(0^\circ)$	0	$\frac{1}{2} e^{-j\theta+3\pi/2}(270^\circ)$	$\frac{1}{2} e^{-j\theta+2\pi}(0^\circ)$
Polarization	HP	VP	RHCP	LHCP

up the signal path for Tx and Rx separately and enables high isolation between Tx and Rx according to proper Tx and Rx polarization pairs. Figure 3 shows the schematic of the switching mode hybrid matrix where P<sub>1</sub>, P<sub>2</sub>, P<sub>3</sub>, and P<sub>4</sub> are input, outputs, and isolation ports, respectively, for the case of Tx. Similarly, P<sub>2</sub> and P<sub>3</sub> become inputs, whereas P<sub>1</sub> and P<sub>4</sub> become output and isolation ports, respectively, for the case of Rx.

As shown in Figure 3, if the incident and reflected voltages at each port are denoted by V<sup>+</sup> and V<sup>-</sup>, the relationships for the switching mode hybrid matrix can be found by

$$\begin{bmatrix} V_2^- \\ V_3^- \end{bmatrix} = \begin{bmatrix} Z_0 & j2X \\ 2X+jZ_0 & 2X+jZ_0 \\ j2X & Z_0 \\ 2X+jZ_0 & 2X+jZ_0 \end{bmatrix} \cdot \begin{bmatrix} V_1^+ \\ V_4^+ \end{bmatrix}, \quad (1)$$

where Z<sub>0</sub> is the characteristic impedance (50 Ω) and X is the load impedance switchable by SP4T. If P<sub>1</sub> and P<sub>2</sub> are used as the input and isolation port (V<sub>4</sub><sup>+</sup> = 0), the output relationship can be expressed as follows,

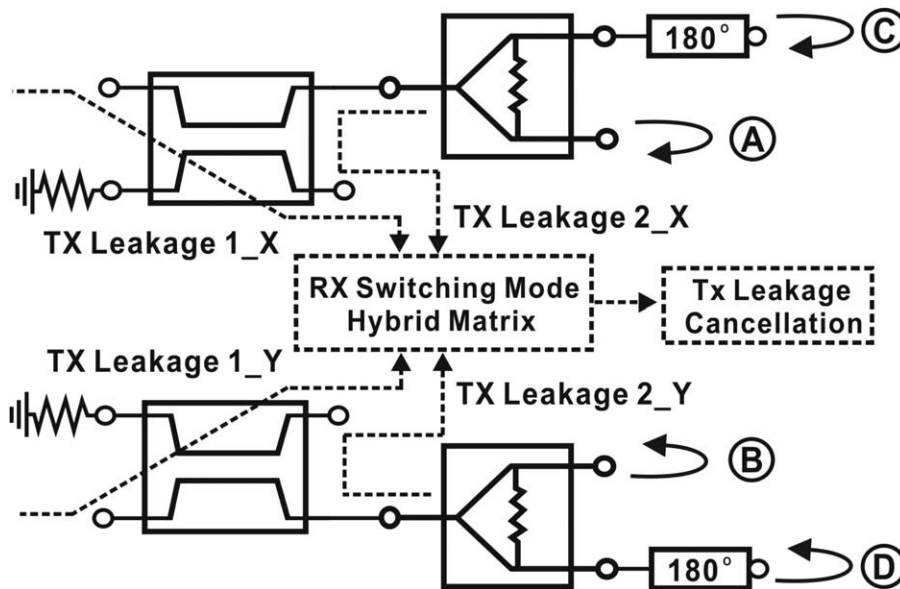


**Figure 6** Tx leakage cancellation for CP modes

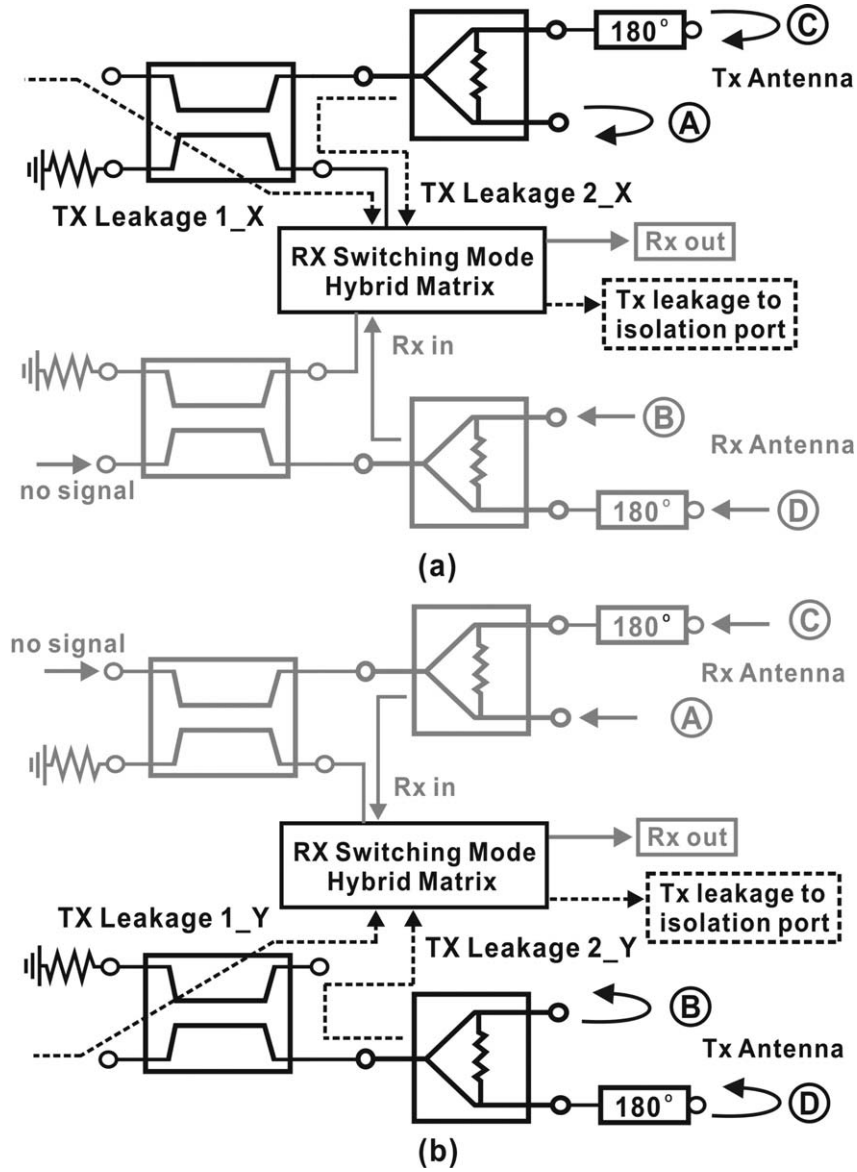


Figure 7 Tx leakage cancellation for LP modes: (a) VP and (b) HP

$$\frac{V_3^-}{V_2^-} = \frac{j2X}{Z_0} \quad (2)$$

When  $X$  equals to  $\infty$  (open), all signals flow to port 3. Similarly, when  $X$  equals to 0 (short), all signals flow to port 2. When  $X$  satisfies  $\omega L = Z_0/2(+j25)$  or  $\omega C = 2/Z_0(-j25)$  the signal gets equally divided into two ports by  $|V_3/V_2|=1$  with  $\angle(S_{31}/S_{21})=90^\circ$  and  $\angle(S_{31}/S_{21})=-90^\circ$ , respectively.

2.2. Analysis for Four-Port Antenna Feeding Network with Switchable Polarizations and Tx/Rx Isolation

Using two switching mode hybrid matrices in combination with two directional couplers and Wilkinson dividers (combiners), the proposed antenna feeding network can be configured to generate switchable polarizations with high Tx/Rx isolations characteristics. Figure 4 shows the description of the proposed antenna feeding network operation. For the transmit-operation, Tx switching mode hybrid matrix determines the signal distribution to Tx outputs with desired phases while Rx switching mode hybrid matrix provides the Tx leakage cancellation path. Similar performance is applied to the receive-operation of the proposed

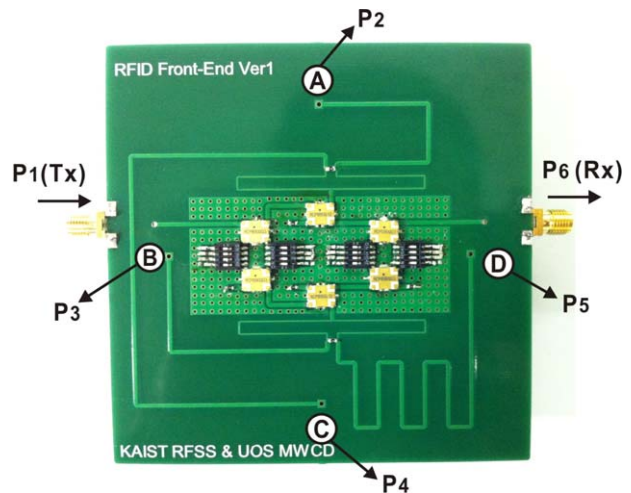
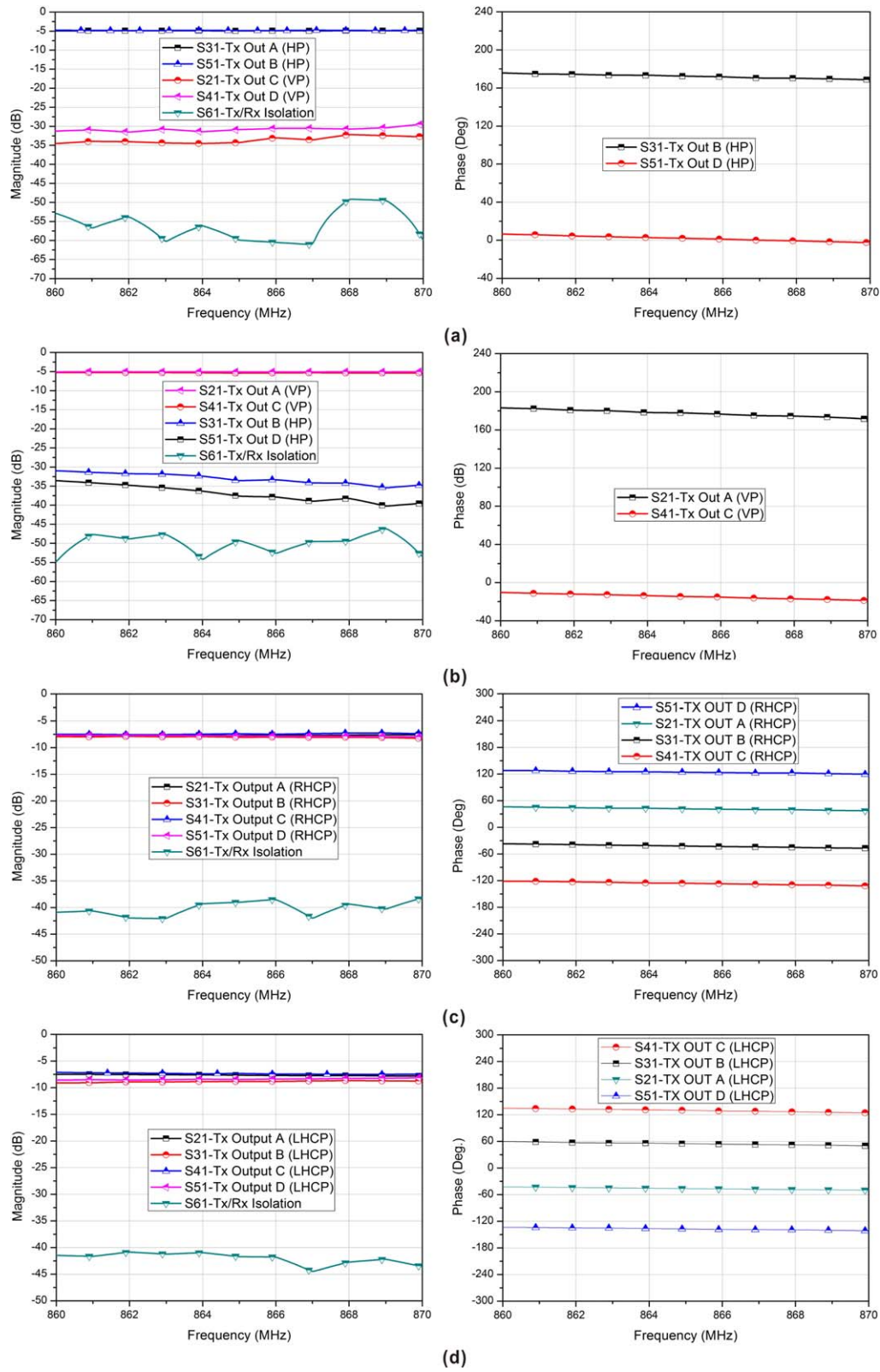


Figure 8 Implementation of the proposed four-port balanced antenna feeding network. [Color figure can be viewed in the online issue, which is available at wileyonlinelibrary.com]



**Figure 9** Measured S-parameters for each operation mode according to switching impedances: (a) HP (open), (b) VP (short), (c) RHCP (+j25), and (d) LHCP (-j25). [Color figure can be viewed in the online issue, which is available at [wileyonlinelibrary.com](http://wileyonlinelibrary.com)]

network by symmetry. If the incident signal on Tx input is assumed to be  $e^{-j\theta}$ , then the relative Tx outputs corresponding to Figure 5 can be summarized as Table 1.

Having the proposed four-port balanced feeding network, a patch antenna can produce different polarizations as shown in

Figure 5. Similarly, the polarizations generated by Rx modes are the same as the Tx polarizations due to the symmetric structure of the proposed feeding network. As the proposed feeding network has switchable and balanced structure, Tx leakages are canceled and isolated, thus high Tx/Rx isolation characteristics

can be maintained. As shown in Figure 6, two types of Tx leakages flow into Rx: Tx Leakage1 and Tx Leakage2. The former directly leaks from Tx input due to the imperfection of directional coupler and the latter reflects from antenna impedance

mismatch and combines through Wilkinson combiner. Considering the symmetry of balanced structure and phase delays by the proposed feeding network, the Tx leakage for circular polarization can be analyzed as

$$\begin{aligned}
 \text{Total Tx Leakage} &= \text{Tx Leakage 1}_{(X+Y)} + \text{Tx Leakage 2}_{(X+Y)} \\
 &= \frac{1}{2} \cdot e^{-j\theta} \cdot \left[ e^{-j\pi/2} + e^{-j3\pi/2} \right] + \frac{1}{2} \cdot \Gamma \cdot e^{-j(\theta+\pi)} \cdot \left[ e^{-j\pi/2} + e^{-j3\pi/2} \right]; & \text{for RHCP}_{\text{TX}}, \text{RHCP}_{\text{RX}} \\
 &= \frac{1}{2} \cdot e^{-j\theta} \cdot \left[ e^{-j3\pi/2} + e^{-j\pi/2} \right] + \frac{1}{2} \cdot \Gamma \cdot e^{-j(\theta+\pi)} \cdot \left[ e^{-j3\pi/2} + e^{-j\pi/2} \right]; & \text{for LHCP}_{\text{TX}}, \text{LHCP}_{\text{RX}} \\
 &= 0 \quad (\text{Tx Leakage cancelled})
 \end{aligned} \tag{3}$$

where all phases are relatively indicated with respect to couplers and dividers (combiners). The detailed effect of antenna load variations on Tx/Rx isolation characteristics for four-port balanced structure is analyzed in Ref. 5, where the operation principles are the same.

For linear polarizations, the switching mode hybrid matrices for Tx and Rx are set to be orthogonal such that polarizations for Tx and Rx are LP (VP) and VP (LP), respectively. As Tx/Rx paths and antennas (vertical and horizontal) are electrically separated by switching mode hybrid matrix, all the Tx leakages flow to the isolation port of Rx and stable isolation characteristics can be achieved as shown in Figure 7.

### 3. MEASUREMENT

Figure 8 shows the implemented four-port balanced antenna feeding network for which A, B, C, and D indicate the feeding points on a patch antenna and correspond to port 2, 3, 4, and 5, respectively. Port 1 and 6 are Tx and Rx ports. The proposed feeding network is implemented with FR4 ( $t=0.6$  mm,  $\epsilon_r=4.6$ ) and total size is  $100 \times 100$  mm<sup>2</sup>. The four-port balanced feeding network is configured by commercially available 3-dB couplers, 10-dB couplers, and SP4T switches. Having additional electrical delays by switches and lines, the open, short,  $+j25$ , and  $-j25$  impedances are experimentally found and realized by lumped chip capacitors and inductors. Finally, the performance of the proposed circuit is verified at European UHF RFID band, 862–868 MHz.

Figure 9 shows the measured  $s$ -parameters for the proposed four-port balanced antenna feeding network corresponding to Figure 8. As shown in Figures 9(a) and 9(b), only two signal paths having 180° phase difference are activated by open or short impedances of the switch and thus horizontal polarization (HP) or LP can be generated with a patch antenna. As shown in Figures 9(c) and 9(d), all four signal paths having quadrature phase differences are activated by  $+j25$  or  $-j25$  impedances, thus, RHCP or LHCP can be generated with a patch antenna with respect to the rotation of quadrature phases. The measured insertion loss variations and phase variations are within  $\pm 1.2$  dB and  $\pm 15^\circ$  from 862 to 868 MHz. Also, the measured Tx/Rx isolation is always better than 38 dB and the measured return losses are always better than 12 dB. As the four-port balanced antenna feeding network is a symmetric structure, Rx operation is the same as the Tx operation.

### 4. CONCLUSION

This article presented a new four-port balanced antenna feeding network for patch antenna applications. The proposed feeding network was able to make four different types of

polarizations (HP, VP, RHCP, and LHCP) by switching impedances of switching mode hybrid matrices with the use of single patch antenna. In addition, high Tx/Rx isolation characteristics stable to antenna impedance variations can be achieved. The implemented four-port balanced antenna feeding network was verified at European UHF RFID band (862–868 MHz). The measured results for the proposed feeding network showed proper distribution of signals according to the switching operations and high isolations characteristics for each operation.

### REFERENCES

1. J. Kim, S. Ko, S. Jeon, J. Park, and S. Hong, Balanced topology to cancel Tx leakage in CW radar, *IEEE Microwave Wireless Compon Lett* 13 (2004), 443–445.
2. C.Y. Kim, J.G. Kim, and S. Hong, A quadrature radar topology with Tx leakage canceller for 24-GHz radar applications, *IEEE Trans Microwave Theory Tech* 55 (2007), 1438–1444.
3. C.Y. Kim, J.G. Kim, D.H. Baek, and S. Hong, A circularly polarized balanced radar front-end with a single antenna for 24-GHz radar applications, *IEEE Trans Microwave Theory Tech* 57 (2009), 293–297.
4. W.G. Lim, S.Y. Park, W.I. Son, M.Q. Lee, and J.W. Yu, RFID reader front-end having robust Tx leakage canceller for load variation, *IEEE Trans Microwave Theory Tech* 57 (2009), 1348–1355.
5. H.L. Lee, W.G. Lim, K.S. Oh, and J.W. Yu, 24 GHz balanced doppler radar front-end with Tx leakage canceller for antenna impedance variation and mutual coupling, *IEEE Trans Antennas Propag* 59 (2011), 4497–4504.

© 2014 Wiley Periodicals, Inc.

## DESIGN OF A MULTILAYERED SIX-APERTURE DIRECTIONAL COUPLER USING SUBSTRATE INTEGRATED WAVEGUIDE

Moustapha Mbaye,<sup>1</sup> Larbi Talbi,<sup>1</sup> and Khelifa Hettak<sup>2</sup>

<sup>1</sup>Department of Computer Science and Engineering, Université du Québec en Outaouais (UQO), 101 Saint-Jean-Bosco, PO Box 1205, Hull Station, Gatineau, QC, J8Y 3G5, Canada; Corresponding author: moustapha.mbaye@uqo.ca

<sup>2</sup>Industry Canada, Communications Research Centre Canada (CRC), 3701 Carling Avenue, Ottawa ON K2H 8S2, Canada

Received 5 April 2013

**ABSTRACT:** The design of a six-aperture, 10-dB directional coupler using substrate integrated waveguide is presented. Size constraints precluded addition of holes in series, however, in parallel the addition